JACS
JOURNAL OF THE AMERICAN CHEMICAL SOCIETY

Communication

pubs.acs.org/JACS

Narrowing the Zero-Field Tunneling Resonance by Decreasing the Crystal Symmetry of Mn_{12} Acetate

Jordi Espín,[†] Ricardo Zarzuela,[‡] Nahuel Statuto,[‡] Jordi Juanhuix,[§] Daniel Maspoch,[†,∥] Inhar Imaz,*[,†] Eugene Chudnovsky,[⊥] and Javier Tejada*[,‡]

[†]Catalan Institute of Nanoscience and Nanotechnology (ICN2), CSIC and The Barcelona Institute of Science and Technology, Campus UAB, Bellaterra, 08193 Barcelona, Spain

[‡]Departament de Física Fonamental, Facultat de Física, Universitat de Barcelona, Martí i Franquès 1, 08028 Barcelona, Spain

[§]Alba Synchrotron Light Facility, 08290 Cerdanyola del Vallés, Barcelona, Spain

[∥]ICREA, Pg Lluís Companys 23, 08100 Barcelona, Spain

[⊥]Physics Department, Lehman College, The City University of New York, 250 Bedford Park Boulevard West, Bronx, New York 10468-1589, United States

Supporting Information

ABSTRACT: We report the discovery of a less symmetric crystalline phase of Mn_{12} acetate, a triclinic phase, resulting from recrystallizing the original tetragonal phase reported by Lis in acetonitrile and toluene. This new phase exhibits the same structure of Mn_{12} acetate clusters and the same positions of tunneling resonances on the magnetic field as the conventional tetragonal phase. However, the width of the zero-field resonance is at least 1 order of magnitude smaller—can be as low as 50 Oe—indicating very small inhomogeneous broadening due to dipolar and nuclear fields.

Chemistry and physics of molecular magnets have been intensively studied in the last two decades[1] after it was found that they provide an ultimate limit of the miniaturization of a permanent magnet[2] and, on top of it, exhibit quantum tunneling of the magnetic moment.[3−6] Other fascinating quantum effects observed in molecular magnets include quantum topological Berry phase,[7] magnetic deflagration,[8,9] and Rabi oscillations.[10,11] Remarkably, recent experiments performed with individual magnetic molecules bridged between conducting leads and molecules grafted on carbon nanotubes have permitted the readout of quantum states of individual atomic nuclei.[12,13] Quantum superposition of spin states in magnetic molecules makes them candidates for qubits, elements of quantum computers.[14]

Among the most studied molecular magnets, Mn_{12} acetate, which was first synthesized by Lis,[15] is a prototypical spin-10 molecular magnet that shows quantum magnetic hysteresis due to resonant spin tunneling.[3] Spin tunneling in a Mn_{12} cluster is illustrated in Scheme 1. The resonances are achieved on changing the external magnetic field B. Their width is due to inhomogeneous dipolar and hyperfine broadening as well as due to D-strains and g-strains.[16] Typically, observed widths of the resonances are in the ballpark of 1 kOe. The zero-field resonance stands out because it is not subject to D-strains and g-strains. It also does not depend on whether one works with a single crystal or nonoriented microcrystals. For conventional

Scheme 1. Thermally Assisted Tunneling between Resonant Spin Levels in a Mn_{12} Cluster of Spin $S = 10$[a]

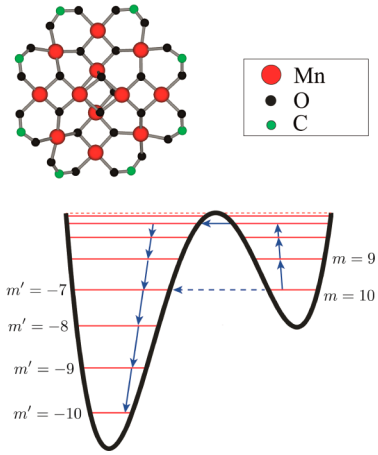

[a]The black solid curve shows the dependence of the classical magnetic anisotropy energy on the angle that the magnetic moment forms with the magnetic anisotropy axis. Red lines show energies of spin levels corresponding to magnetic quantum numbers m and m'. The dash line illustrates quantum tunneling from $m = 10$ to $m' = -7$.

Mn_{12} acetate, the typical width of the zero-field resonance is in the ballpark of 300 Oe.[17] Inhomogeneous broadening of spin-tunneling resonances is one obstacle on the way to achieving terahertz lasing and superradiance effects in molecular magnets.[18,19] Herein we report the discovery of a less symmetric crystalline phase (triclinic phase) of Mn_{12} acetate that exhibits surprisingly narrow width of the zero-field resonance, which, in some instances, can be as low as 50 Oe.

Recently, we reported spin-tunneling maxima in the field derivative of the magnetization of amorphous nonoriented Mn_{12} acetate nanospheres.[20] This observation challenged the conventional wisdom that quantum resonances can only be

Received: May 25, 2016
Published: July 6, 2016

DOI: 10.1021/jacs.6b05380
J. Am. Chem. Soc. 2016, 138, 9065−9068

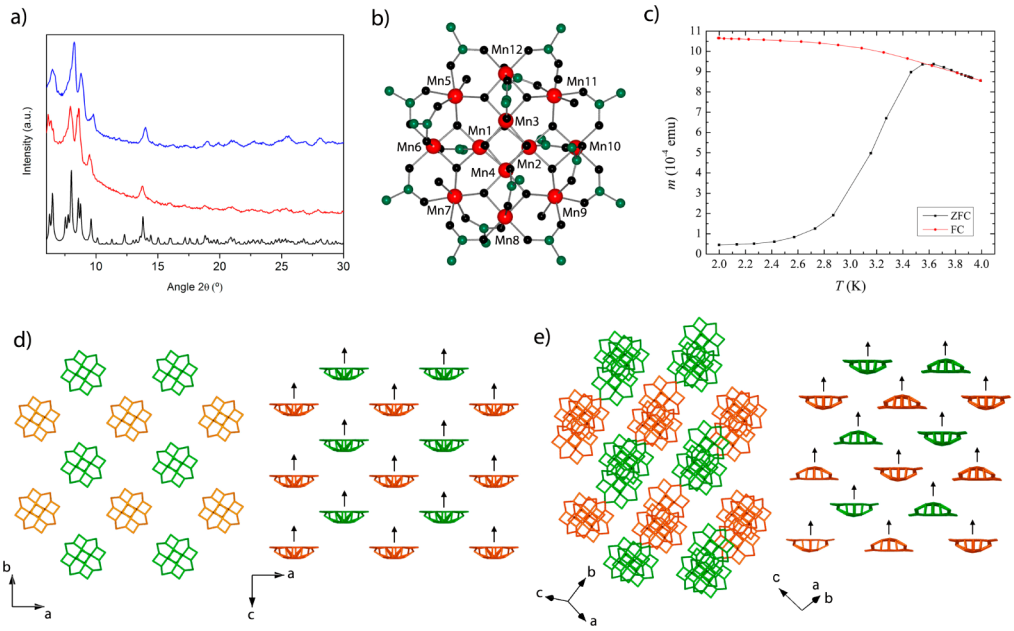

Figure 1. (a) XRPD of the $\mathbf{Mn_{12\_triclinic}}$ microribbons (blue) and the single crystals of $\mathbf{Mn_{12\_triclinic}}$ (red), as compared to the simulated powder pattern for the crystal structure of $\mathbf{Mn_{12\_triclinic}}$. (b) View of the Mn_{12} acetate cluster in $\mathbf{Mn_{12\_triclinic}}$. (c) ZFC (black) and field-cooled (red) magnetization vs temperature for a sample of $\mathbf{Mn_{12\_triclinic}}$ at H = 100 Oe. A single peak indicates the absence of any second species of Mn_{12} clusters. (d,e) Comparison between the arrangement of Mn_{12} acetate clusters in the tetragonal (d) and triclinic (e) phases. Arrows (conceptual) show the directions of the easy magnetization axes of the clusters. Note that the Mn_{12} acetate clusters are aligned along their easy magnetization axes in the tetragonal phase, whereas they are not in the triclinic phase, and that acetate ligands and toluene and water molecules have been omitted for clarity.

observed in single crystals or in systems of oriented microcrystals. The amorphous Mn_{12} acetate spheres were prepared by initially dissolving single crystals of Mn_{12} acetate corresponding to the tetragonal phase reported by Lis[15] in acetonitrile.[21] Then, this solution was added into a toluene solution to provoke a fast precipitation of a brown solid. Finally, the resulting mixture was filtrated by conventional filtering paper, and the Mn_{12} acetate nanospheres were collected by centrifugation (8000 rpm during 4 min) of the filtrate. In this process, a surprising observation was that the initial collected brown solid was crystalline and that the X-ray powder diffraction showed a different pattern to that exhibited by the tetragonal Mn_{12} acetate crystals (see Figure S1).[15] Field-emission scanning electron microscope images of this brown crystalline powder revealed the formation of ribbon-like microcrystals (width: 0.8 ± 0.3 μm, length: 3.2 ± 1.9 μm; see Figure S2).

To identify this new crystalline phase, the reaction was slowed down by diffusing toluene vapors over a solution resulting from dissolving the tetragonal Mn_{12} acetate crystals in acetonitrile. After 3 days, small brown rectangular plate-like crystals suitable to perform single-crystal diffraction experiments using synchrotron radiation were obtained (see Figure S3). The new Mn_{12} phase (hereafter called $\mathbf{Mn_{12\_triclinic}}$) crystallizes in the $P\bar{1}$ space group; in contrast to the tetragonal $I\bar{4}$ space group of the original Mn_{12} acetate reported by Lis (Figure 1a; see Table S1).[15] In comparison to the initial tetragonal phase, the structure of the $Mn_{12}O_{12}(O_2CCH_3)_{16}(H_2O)_4$ cluster in this new crystalline phase is preserved (Figure 1b). The asymmetric unit contains 12 Mn atoms exhibiting octahedral coordination geometry. Two different environments for the Mn atoms can be observed. The four central Mn^{4+} (Mn1−Mn4) are situated in the core of the structure forming a cubic oxocluster $[Mn_4O_4]^{8+}$, where each Mn^{4+} is coordinated to one oxygen atom from an acetate group and five bridging oxygen atoms. Surrounding the central Mn^{4+} oxocluster, there are eight more Mn^{3+} atoms (Mn5−Mn12) held within a nonplanar ring by eight oxygen atoms. Half of these Mn^{3+} atoms (Mn5, Mn7, Mn9, and Mn11) coordinate to three oxygen atoms from three different acetate groups, to one oxygen atom from a water molecule, and to two bridging oxygen atoms. The remaining four Mn^{3+} atoms (Mn6, Mn8, Mn10, and Mn12) coordinate to four oxygen atoms from four different acetate groups and to two bridging oxygen atoms. The 16 acetates are oriented in two different directions: in axial (four pointing up and four pointing down) and equatorial (eight acetates) directions.

The main difference between $\mathbf{Mn_{12\_triclinic}}$ and the tetragonal phase resides in the presence of intercalated toluene solvent molecules (Figure S4) as well as in the intermolecular packing of the Mn_{12} acetate clusters. Comparing both phases, the Mn_{12} acetate clusters in the more symmetric tetragonal phase show an overlap alignment along the *a*, *b*, and *c* axes. This latter corresponds to the alignment of the easy magnetization axes of the Mn_{12} acetate clusters (Figure 1d). However, this perfect alignment of the easy magnetization axes of the clusters is lost in $\mathbf{Mn_{12\_triclinic}}$ (Figure 1e). This phase only shows an overlap alignment of the clusters along the $\langle 1\bar{1}0\rangle$ and $\langle \bar{1}10\rangle$ directions.

To investigate the magnetic properties of $\mathbf{Mn_{12\_triclinic}}$, we first carried out low-temperature magnetic measurements on a compressed powdered sample inside a commercial rf-SQUID Quantum Design magnetometer. Figure 1c shows zero-field-cooled (ZFC) magnetization as a function of temperature. The maximum at about 3.5 K corresponds to the conventional blocking temperature of the Mn_{12} acetate cluster. Below this temperature, the clusters hold their magnetic moments, while above this temperature, they become superparamagnetic. The absence of any secondary maxima in the ZFC curve indicates

DOI: 10.1021/jacs.6b05380
J. Am. Chem. Soc. 2016, 138, 9065−9068

the presence of only one species of Mn_{12} acetate having fixed magnetic anisotropy energy of about 65 K. Hysteresis loops of the magnetization taken at different temperatures are shown in Figure 2a. The corresponding descending branches are

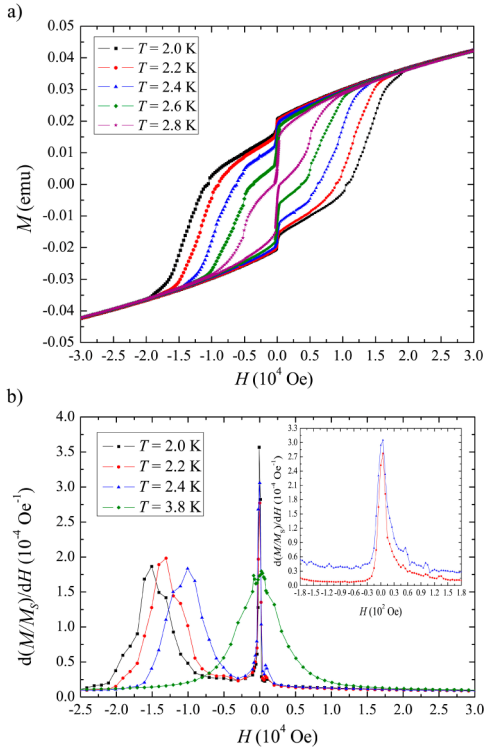

Figure 2. (a) Hysteresis loops of the magnetization of $\mathbf{Mn_{12\_triclinic}}$ taken at different temperatures. The data along the descending branch are obtained by saturating the sample in a positive field and reducing and reversing the magnetic field. The curves show large jumps at zero field that have not been previously observed in Mn_{12} Lis phase. (b) $d(M/M_s)/dH$ along the descending branch of $\mathbf{Mn_{12\_triclinic}}$ at different temperatures. Spin-tunneling maxima at zero and first resonant fields are clearly observed. Inset shows low-field structure of the zero-field maximum at 2.2 and 2.4 K in steps of 5 Oe.

obtained by first saturating $\mathbf{Mn_{12\_triclinic}}$ in a positive magnetic field of up to 3 T and then reducing the magnetic field to zero, reversing it, and increasing the field in the opposite direction at a constant rate. Analogous protocol is carried out for the ascending branches. Striking feature of these magnetization curves is a very large narrow jump of the magnetization at zero field for both ascending and descending protocols. In the past, such jumps have only been seen in a large magnetic field due to the phenomenon of magnetic deflagration.[8,9] The latter is equivalent to chemical combustion: reversal of the magnetic moments of the molecules leads to the release of their Zeeman energy into heat that further enhances magnetic relaxation. However, at $B = 0$, there is no Zeeman energy to burn, so that the deflagration as an explanation to the jumps is ruled out. The derivative of the normalized magnetization, $d(M/M_s)/dH$, along the descending branch is shown at different temperatures in Figure 2b. It clearly indicates four tunneling maxima at the conventional resonant fields of Mn_{12} acetate, separated by about 0.46 T. Analogous behavior is observed for the ascending protocol. The presence of such maxima in $d(M/M_s)/dH$ of nonoriented amorphous particles of a molecular magnet has been explained in a previous study.[18] The new feature is an extremely narrow width of the zero-field maximum. In some instances, it is below 50 Oe (Figure 2b, inset). Such a narrow spin tunneling resonance has never been observed in any molecular magnet.

In accordance with the narrow width of the zero-field resonance, one finds an unusually fast magnetic relaxation near-zero field (Figure 3). A single exponential provides a good fit to

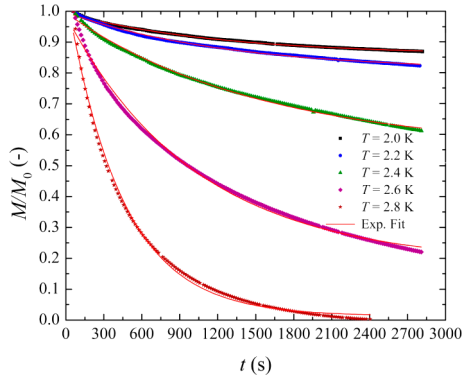

Figure 3. Exponential time relaxation of the normalized magnetization in a field of −20 Oe at different temperatures from 2.0 to 2.8 K in increments of 0.2 K.

the time dependence of the magnetic moment of the sample at all temperatures explored (2.0−2.8 K), with mean lifetimes ranging from ∼438 to 1530 s. This means that a single energy barrier contributes to the relaxation. It is determined by the distance from the ground-state level E_0 to the level E_m that dominates thermally assisted quantum tunneling (Scheme 1).

The jump in the magnetization due to resonant spin tunneling is determined by the incoherent Landau−Zener process.[22] The initial, M_i, and the final, M_f, magnetizations are connected through $M_i/M_f = \exp\{\pi\Delta_m^2 \exp[-(E_0 - E_m)/T]/(2\upsilon)\}$, where Δ_m is the tunnel splitting of the level m that dominates thermally assisted quantum tunneling, and $\upsilon = 2m\mu_B(dB/dt)$ is the rate at which Zeeman energy is changing due to the field sweep, μ_B being the Bohr magneton. The double exponential dependence on temperature provides a hint as to why the size of the magnetization jump in Figure 2a increases sharply with a relatively small increase of temperature. An additional proof of the Landau−Zener dynamics of the magnetization comes from the analysis of the experiment in which the field sweep near-zero field on a field reduction from saturation was conducted in equal field steps, with a sizable magnetization change after each step and a little change between the steps. For two consecutive steps, one has $(M_{i,n}/M_{f,n})\,(M_{i,n+1}/M_{f,n+1}) = M_{i,n}/M_{f,n+1}$, where $M_{i,n+1} = M_{f,n}$ has been used. Writing $(dB/dt)_n$ as $\Delta B/\Delta t_n$, one obtains after N steps:

$$\frac{M_i}{M_f} = e^{(\pi\Delta_m^2 e^{-(E_0-E_m)/T}/4m\mu_B\Delta B)t}, \quad t = \Delta t_1 + \Delta t_2 + \ldots + \Delta t_N$$

resulting in $\ln(M_i/M_f) \propto t$. The linear time dependence of $\ln(M_i/M_f)$ observed in experiment is illustrated by Figure 4.

The width of the zero-field resonance is determined by the inhomogeneous broadening due to dipole−dipole interaction between magnetic moments of the Mn_{12} acetate clusters and due to hyperfine interactions that are rather strong in Mn_{12}. Strong dipolar broadening in conventional tetragonal crystals of Mn_{12} acetate is due to the tendency of the clusters to form ordered chains along the tetragonal c axis. This tendency should

DOI: 10.1021/jacs.6b05380
J. Am. Chem. Soc. 2016, 138, 9065−9068

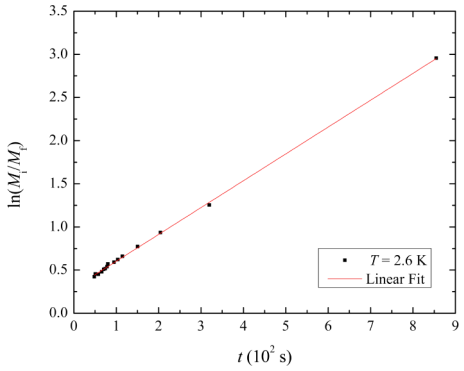

Figure 4. Linear time dependence of $\ln(M_i/M_f)$ during a stepwise field sweep at T = 2.6 K.

be greatly diminished in the triclinic structure. In the new crystal phase $\mathbf{Mn_{12\_triclinic}}$ reported here, the magnetic moments of the clusters do not perfectly overlap (Figure 1e). Still it appears unlikely that the dipolar broadening in $\mathbf{Mn_{12\_triclinic}}$ would fall below 50 Oe. Even if the dipolar broadening of the resonance is very low, the question would remain about the absence of the hyperfine broadening, which should be on the order of a few hundred Oe. One possible explanation to the data is provided by recent theoretical work that shows that the magnetization reversal in a molecular magnet may occur inside a front of quantum tunneling moving through the sample. This may happen either due to the formation of a domain wall with a zero dipolar bias inside the wall[23] or due to the formation of a self-organized front of quantum tunneling with zero bias between tunneling spin levels regardless of the nature of inhomogeneous broadening.[24] The latter effect presents the most interesting possibility. It is similar to the optical laser effect: The dipolar field in a system of magnetic dipoles self-organizes to provide the fastest relaxation to the minimum energy state. It has been demonstrated[24] that self-organization of dipolar field can provide the resonant condition in the presence of a very significant (up to 25%) broadening of the energy of spin levels. Further studies will reveal if self-organization is the reason for the observed narrow zero-field resonance. If it is, it may open the way to lasing with molecular magnets in the terahertz frequency range.

■ ASSOCIATED CONTENT

Supporting Information

The Supporting Information is available free of charge on the ACS Publications website at DOI: 10.1021/jacs.6b05380.

Crystallographic data (CIF)
Synthesis, XRPD, crystallographic table, SEM images. CCDC number is 1479959 (PDF)

■ AUTHOR INFORMATION

Corresponding Authors

*inhar.imaz@icn2.cat
*jtejada@ubxlab.com

Notes

The authors declare no competing financial interest.

■ ACKNOWLEDGMENTS

The work at the University of Barcelona has been supported by MINECO Project MAT2011-23698. J.E. thanks the MINECO for a FPI fellowship. The work of E.M.C was supported by the U.S. National Science Foundation; grant DMR-1161571. ICN2 acknowledges the support of the Spanish MINECO through the Severo Ochoa Centers of Excellence Program; grants SEV-2015-0496 and SEV-2013-0295.

■ REFERENCES

(1) *Molecular Magnets – Physics and Applications*; Bartolomé, J., Luis, F., Fernández, J. F., Eds.; Springer: Heidelberg, 2014.
(2) Sessoli, R.; Gatteschi, D.; Caneschi, A.; Novak, M. A. *Nature* **1993**, *365*, 141.
(3) Friedman, J. R.; Sarachik, M. P.; Tejada, J.; Ziolo, R. *Phys. Rev. Lett.* **1996**, *76*, 3830.
(4) Hernandez, J. M.; Zhang, X. X.; Luis, F.; Bartolome, J.; Tejada, J.; Ziolo, R. *Europhys. Lett.* **1996**, *35*, 301.
(5) Thomas, L.; Lionti, F.; Ballou, R.; Gatteschi, D.; Sessoli, R.; Barbara, B. *Nature* **1996**, *383*, 145.
(6) Chudnovsky, E. M.; Tejada, J. *Macroscopic Quantum Tunneling of the Magnetic Moment*; Cambridge University Press: Cambridge, 1998.
(7) Wernsdorfer, W.; Sessoli, R. *Science* **1999**, *284*, 133.
(8) Suzuki; Sarachik, M. P.; Chudnovsky, E. M.; McHugh, S.; Gonzalez-Rubio, R.; Avraham, N.; Myasoedov, Y.; Zeldov, E.; Shtrikman; Chakov, N. E.; Christou, G. *Phys. Rev. Lett.* **2005**, *95*, 147201.
(9) Hernandez-Minguez, A.; Hernandez, J. M.; Macia, F.; Garcia-Santiago, A.; Tejada, J.; Santos, P. V. *Phys. Rev. Lett.* **2005**, *95*, 217205.
(10) Schlegel, C.; van Slageren, J.; Manoli, M.; Brechin, E. K.; Dressel, M. *Phys. Rev. Lett.* **2008**, *101*, 147203.
(11) Bertaina, S.; Gambarelli, S.; Mitra, T.; Tsukerblat, T.; Müller, A.; Barbara, B. *Nature* **2008**, *453*, 203; *Nature* **2010**, *466*, 1006.
(12) Ganzhorn, M.; Klyatskaya, S.; Ruben, M.; Wernsdorfer, W. *Nat. Nanotechnol.* **2013**, *8*, 165.
(13) Ganzhorn, M.; Klyatskaya, S.; Ruben, M.; Wernsdorfer, W. *ACS Nano* **2013**, *7*, 6225.
(14) Tejada, J.; Chudnovsky, E. M.; del Barco, E.; Hernandez, J. M.; Spiller, T. P. *Nanotechnology* **2001**, *12*, 181.
(15) Lis, T. *Acta Crystallogr., Sect. B: Struct. Crystallogr. Cryst. Chem.* **1980**, *36*, 2042.
(16) Park, K.; Novotny, M. A.; Dalal, N. S.; Hill, S.; Rikvold, P. A. *Phys. Rev. B: Condens. Matter Mater. Phys.* **2001**, *65*, 014426.
(17) Friedman, J. R.; Sarachik, M. P.; Ziolo, R. *Phys. Rev. B: Condens. Matter Mater. Phys.* **1998**, *58*, R14729.
(18) Chudnovsky, E. M.; Garanin, D. A. *Phys. Rev. Lett.* **2002**, *89*, 157201.
(19) Tejada, J.; Amigo, R.; Hernandez, J. M.; Chudnovsky, E. M. *Phys. Rev. B: Condens. Matter Mater. Phys.* **2003**, *68*, 014431.
(20) Lendínez, S.; Zarzuela, R.; Tejada, J.; Terban, M. W.; Billinge, S. J. L.; Espin, J.; Imaz, I.; Maspoch, D.; Chudnovsky, E. M. *Phys. Rev. B: Condens. Matter Mater. Phys.* **2015**, *91*, 024404.
(21) Imaz, I.; Luis, F.; Carbonera, C.; Ruiz-Molina, D.; Maspoch, D. *Chem. Commun.* **2008**, 1202.
(22) Garanin, D. A.; Chudnovsky, E. M. *Phys. Rev. B: Condens. Matter Mater. Phys.* **2002**, *65*, 094423.
(23) Garanin, D. A.; Chudnovsky, E. M. *Phys. Rev. B: Condens. Matter Mater. Phys.* **2008**, *78*, 174425.
(24) Garanin, D. A.; Chudnovsky, E. M. *Phys. Rev. Lett.* **2009**, *102*, 097206.

DOI: 10.1021/jacs.6b05380
J. Am. Chem. Soc. 2016, 138, 9065–9068